




Graphene assembled film based conformal sensor array for submillimeter crack location and direction detection

Huijuan Guan^{1,2†}, Rongguo Song^{1,2†}, Cong Tong^{1,2}, Xin Zhao^{1,2}, Yingping Yang^{1,2*}, and Daping He^{1,2*} 

¹Hubei Engineering Research Center of RF-Microwave Technology and Application, Wuhan University of Technology, Wuhan 430070, People's Republic of China

²Department of Physics, School of Science, Wuhan University of Technology, Wuhan 430070, People's Republic of China

*E-mail: ypyang@whut.edu.cn; hedaping@whut.edu.cn

†These authors contributed equally to this work.

Received November 28, 2022; revised December 20, 2022; accepted January 9, 2023; published online January 30, 2023

In this paper, a conformal CSRR derived sensor array with two resonant frequencies based on a graphene assembled film (GAF) is proposed to detect and determine the direction of submillimeter cracks on aluminum plates. The GAF sensor array consists of a microstrip line, a dielectric substrate and a reference ground with two CSRR derived resonant structures. The GAF sensor array has a high sensitivity of 270 MHz for the curved aluminum plate with a crack width of 0.2 mm. In addition, the CSRR derived resonant structure array of the GAF sensor effectively detects the direction of the crack. © 2023 The Japan Society of Applied Physics

Due to the influence of fatigue loading and other factors, fatigue cracks and other defects are inevitably produced on metal structures.¹⁾ Fatigue cracks often appear in the stressed part of a flat metal structure or in the stressed part of a bent metal structure. The initial location and cracking trend detection of a millimeter or even submillimeter fatigue cracks in time can effectively avoid catastrophic accidents.

The most commonly used non-destructive detection methods include ultrasonic, eddy current, and magnetic leakage detection, which do not achieve real-time monitoring.^{2–4)} In recent years, various radio frequency (RF) sensors have been proposed to detect cracks on metal surfaces.^{5–7)} Compared with other sensors, RF sensors have the advantages of small size, simple data processing, and low cost.⁸⁾ In 2012, Albishi et al. first proposed complementary splitting resonator (CSRR) based sensors for the detection of metal cracks. A CSRR structure has a strong and concentrated electromagnetic field distribution in resonance. Perturbation of the field distribution can cause an obvious resonant frequency shift of CSRR. The sensor showed a frequency offset of about 260 MHz for the crack with a width of 0.2 mm and a depth of 2 mm.⁹⁾ But single-resonance-based RF resonators cannot determine the direction of the crack. In 2019, Dong et al. proposed a wireless passive sensor based on a microstrip antenna constructed by a ceramic substrate and a metal silver paste. The sensor exhibited sensitivities of 3.5 MHz/0.1 mm and 4.5 MHz/0.1 mm for horizontal and vertical cracks, respectively.¹⁰⁾ The rectangular patch antenna sensor can detect the crack direction, but the sensitivity of detecting sub-millimeter cracks is relatively insufficient. In addition, these sensors are mostly based on rigid material designs, thus are only suitable for planar structures with no curvatures.^{11,12)} In 2022, Wang et al. proposed a novel sensor tag based on a split ring resonator with very thin copper that can easily cover the surface of a curved metal structure. For submillimeter cracks, the label exhibited a frequency offset of more than 260 MHz.¹³⁾ However, the sensor with a large physical size and high operating frequency cannot judge the crack direction. More importantly, the resonant frequency offset of the CSRR sensor caused by the crack width and crack depth are in opposite directions. As a result, for cracks with a certain width and depth, the frequency offset is not obvious, and even the phenomenon of missing detection occurs.

Moreover, metal materials based sensors have poor corrosion resistance, which makes the sensor unable to work stably in harsh environments for a long time.

Graphene based films have excellent electrical conductivity and corrosion resistance, and show good electrical stability under mechanical deformation.^{14–17)} Graphene assembled film (GAF) has been widely used in wearable antennae, communication antennae, pressure sensors, and other RF devices.^{18–20)} Meanwhile, in our previous work, a GAF-based conformal rectangular patch antenna sensor was proposed to detect cracks on curved metal surfaces with a sensitivity of 36.82 MHz mm⁻¹, which is sufficient for millimeter cracks.²¹⁾ For the submillimeter cracks, the detection sensitivity needs to be further improved.

In this paper, a conformal CSRR derived sensor array with two resonant frequencies based on GAF is proposed to detect and determine the direction of submillimeter cracks on aluminum plates. The GAF sensor array has a frequency offset of up to 270 MHz for the curved aluminum plate with a crack width of 0.2 mm, which is effective to make a timely warning of the incipient fatigue crack. In addition, the two CSRR derived structures can determine the direction of the crack. Furthermore, the GAF-based conformal sensor array can detect the surface condition of metal structures with various bending radii, making up for the shortcomings of traditional rigid sensors.

In order to avoid the missed detection problem of the traditional CSRR sensor, a CSRR derived structure is designed as shown in Fig. 1(a). The resonant structure consists of a connecting bridge connected to the reference ground, two open rings, and two branches inside. The parameters of the resonant structure are shown in Table I. Figure 1(b) shows the current distribution of the CSRR derived structure, which is closer to the toroidal current than the semi-toroidal current of the traditional CSRR structure, which can achieve omnidirectional detection. Due to the near-field action of the sensor, the metal surface to be tested generates an induced current in the opposite direction of the sensor current. When a fatigue crack appears on the surface of the metal, the induced current distribution is affected, so that the mutual inductance between the metal to be tested and the sensor is weakened, and visually manifested as a deviation in the resonant frequency.

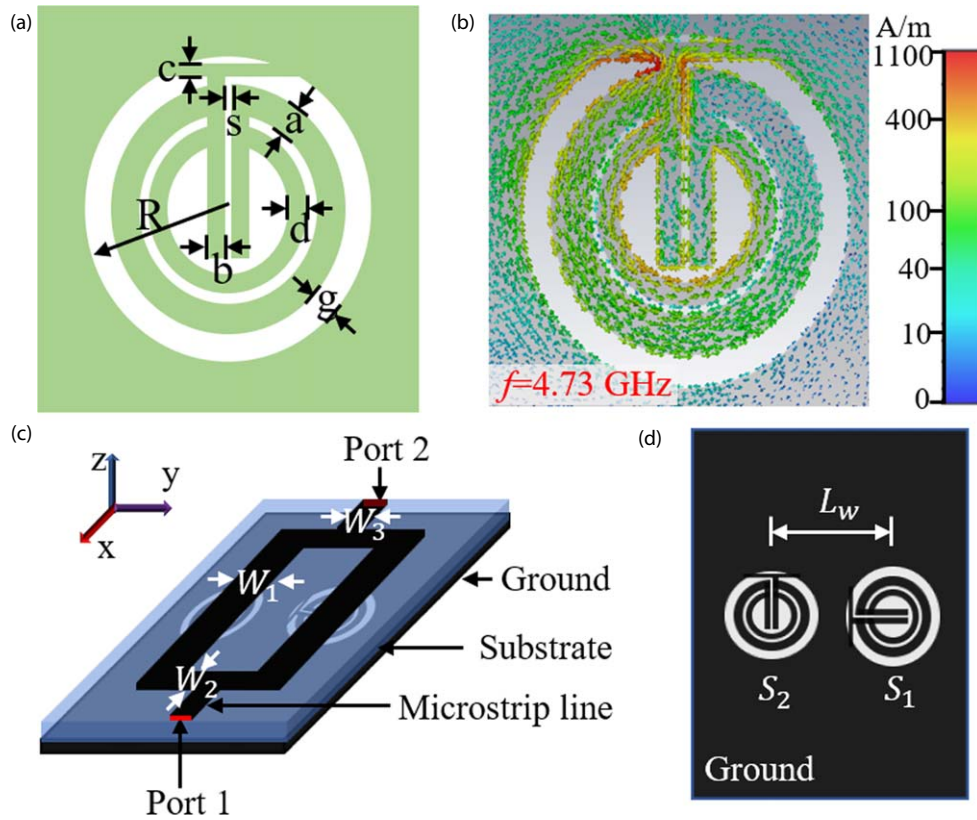


Fig. 1. (Color online) (a) Schematic diagram of CSRR derived structure. (b) Current distribution of CSRR derived structure. (c) The structure of GAF sensor array. (d) Bottom view of GAF sensor array.

Table I. Parameters of GAF sensor array structure.

Parameter	Values (mm)	Parameter	Values (mm)
a	0.5	g	0.4
b	0.3	s	0.1
c	0.2	R_1	2.18
d	0.3	R_2	2
W_1	3	W_2	1.14
W_3	1.14	L_w	10

As shown in Fig. 1(c), the GAF sensor array consists of three layers, including a microstrip line, dielectric substrate, and reference ground. The microstrip line and reference ground are made by GAF with excellent mechanical flexibility and corrosion resistance. The substrate is PET with a

thickness of 0.5 mm and a dielectric constant of 3.5. The three layers of the sensor are designed with flexible materials, which can conformal with bent metal structures and detect cracks. The bottom view of the GAF sensor array is shown in Fig. 1(d). In order to achieve dual frequency, the radius of the two resonant structures (marked S_1 and S_2) is 2.18 mm and 2 mm, respectively. Due to the structural asymmetry, for the single resonant structure, the detection sensitivity of each direction is different. In order to maximize the crack detection sensitivity and make the crack direction judgment more obvious, the orientation of the two resonant structures is vertical, as shown in Fig. 1(d).

In order to explore the performance of detecting cracks on metal surfaces, the GAF sensor based on the CSRR derived structure array is modeled and simulated by CST STUDIO

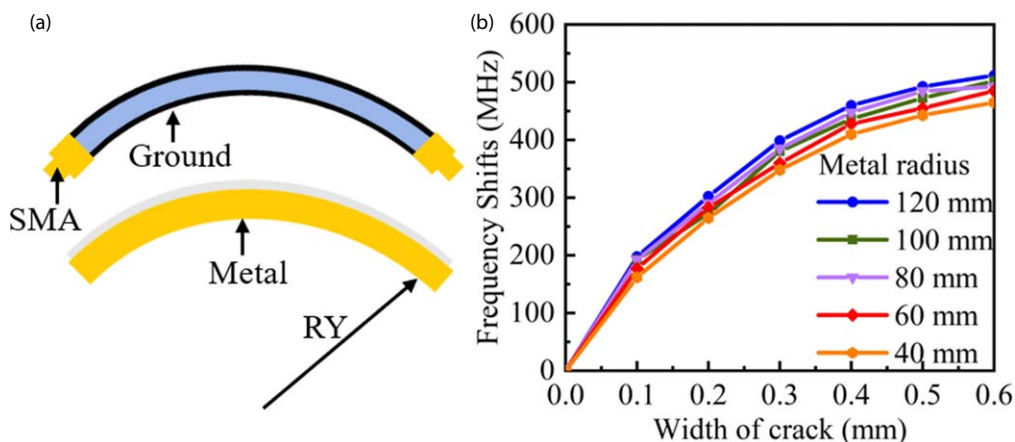


Fig. 2. (Color online) (a) Schematic diagram of conformation GAF sensor array and curved metal structure. (b) Influence of bending radius on crack width detection.

SUITE. As shown in Fig. 2(a), when detecting cracks on the surface of curved metal, the GAF sensor array is bent in the direction of the reference ground and placed on the metal. Figure 2(b) shows the change of frequency offset of the GAF sensor array for detecting crack width extension at different bending radii of 40 mm, 60 mm, 80 mm, 100 mm, and 120 mm, respectively. The length and depth of the crack are 30 mm and 2 mm, respectively. The simulated results of the GAF sensor array at different states have the same trend, and there is little difference in frequency offset under the same crack width.

An aluminum plate with a bending radius of 100 mm is taken as an example to evaluate the detection ability of the GAF sensor array on the width and depth of surface cracks. The length of the crack is 30 mm. Cracks with a depth of 1 mm and varying widths of 0, 0.1, 0.2, and 0.3 mm are designed. The simulated transmission coefficient results of the GAF sensor array to detect different cracks are shown in Fig. 3(a). When the crack appears under the S_1 resonant structure, the resonant frequency f_l will shift, while the resonant frequency f_h will hardly be affected. As the crack width expands, the resonant frequency f_l continues to shift to the low frequency. When the crack depth is expanded from 0 mm to 2 mm by a step of 0.2 mm, the average detection sensitivity of the GAF sensor array to crack depth is shown in Fig. 3(b). Equation (1) is the calculation method of sensor sensitivity, where f is the resonant frequency of the sensor without a crack, f' is the resonant frequency of the sensor with a crack, and p is the crack parameter detected. Similarly, as shown in Fig. 3(c), the crack depth expansion also shifts the resonant frequency to the lower frequency. When the crack width is expanded from

0 mm to 0.6 mm by a step of 0.04 mm, the average detection sensitivity is shown in Fig. 3(d). The average detection sensitivity of the GAF sensor array decreases gradually with the crack depth or width, which indicates that the GAF sensor has high detection sensitivity for sub-millimeter cracks.

$$\text{Sensitivity} = \frac{|f - f'|}{p} \quad (1)$$

In addition, the GAF sensor array based on CSRR derived structure has high accuracy in detecting the crack position and direction. It can be seen from Figs. 4(a) and 4(b) that when the crack on a flat aluminum plate only appears below the resonant structure S_1 , the frequency f_l of the GAF sensor array shifts left, while the resonant frequency f_h does not shift. Similarly, when the crack appears below the resonant structure S_2 , it only affects the resonant frequency f_h . As shown in Figs. 4(c) and 4(d), when cracks appear below two resonant structures, resonant frequencies f_l and f_h both shift to left. Therefore, the crack direction can be determined according to the resonant frequency of the GAF sensor array.

In order to verify the validity of the simulation results, the sensor array based on GAF is fabricated for testing. Figure 5(a) shows the digital photo of GAF with bending and folding state, which indicates excellent flexibility and foldability. The cross-section scanning electron microscope (SEM) image [Fig. 5(b)] shows that the GAF is composed of multiple monolayers of graphene tightly stacked, with a thickness of 24 μm . The fabricated GAF sensor array is shown in Fig. 5(c). The GAF is attached to the flexible PET substrate. The resonant structure and microstrip line are formed by a laser engraving machine in one step. The GAF

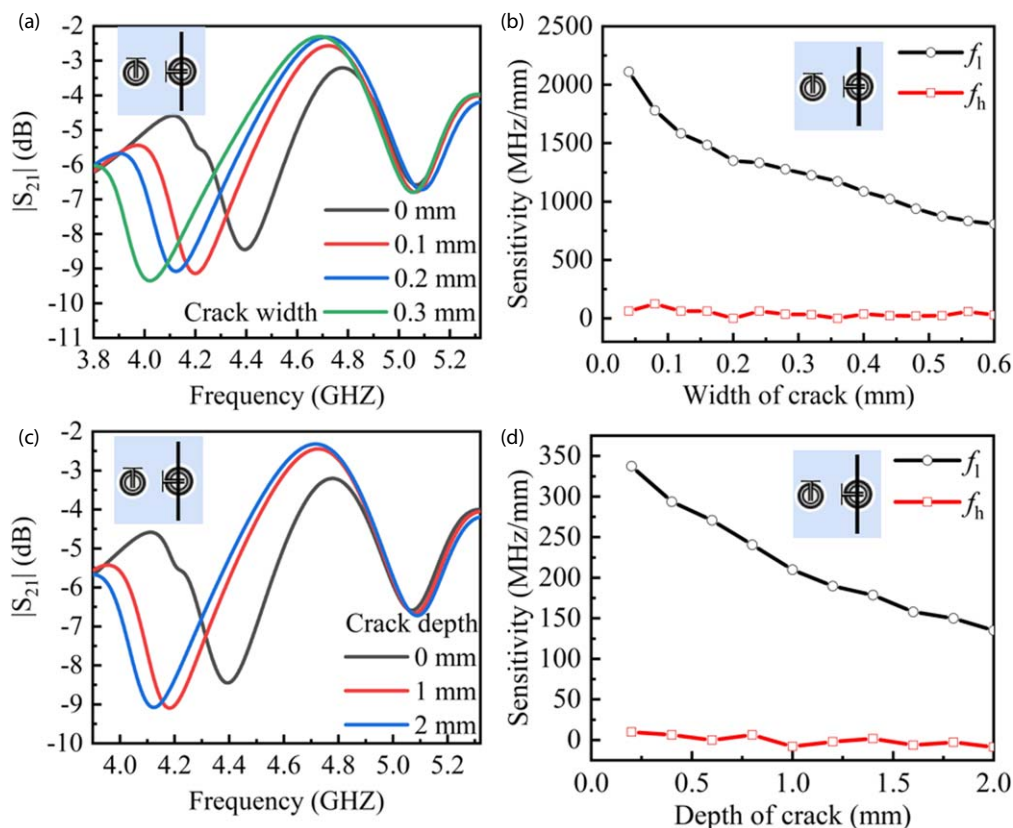


Fig. 3. (Color online) (a) Transmission coefficient of the GAF sensor array corresponding to different crack widths. (b) Average sensitivity of crack depth detection. (c) The transmission coefficient of the GAF sensor array corresponding to different crack depths. (d) Average sensitivity of crack width detection.

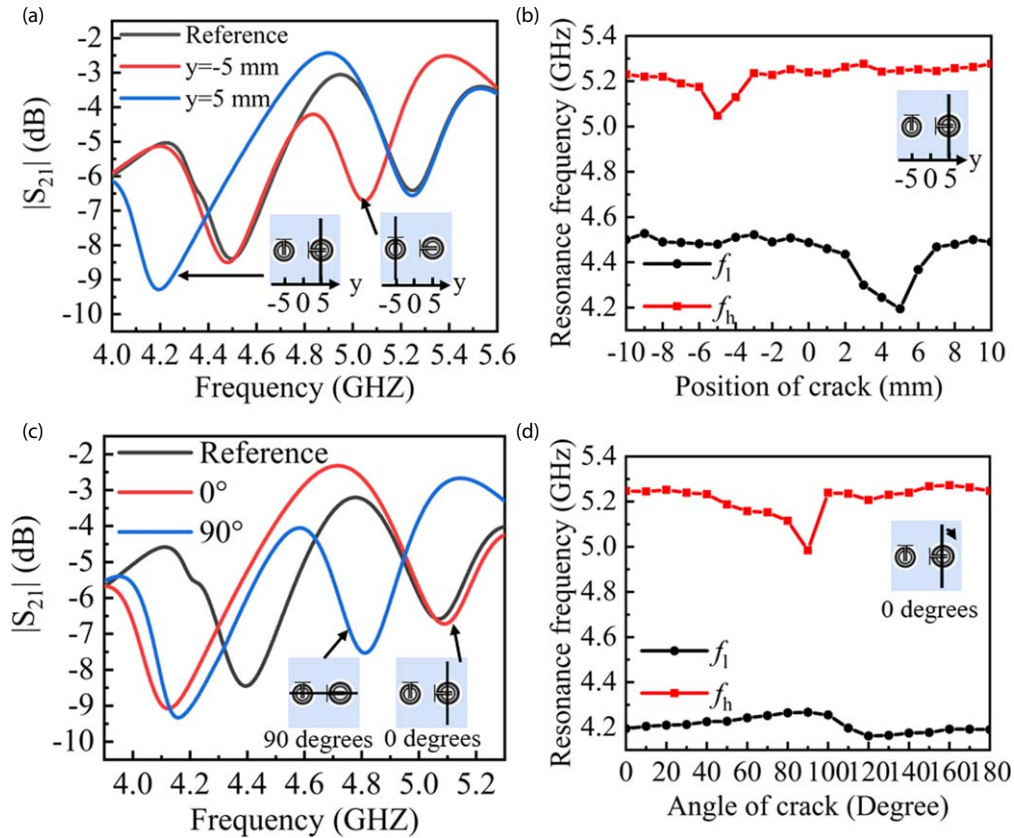


Fig. 4. (Color online) (a) Transmission coefficient of GAF sensor array for crack position scanning. (b) The simulation results of detecting the cracks at different positions. (c) Transmission coefficient for crack direction scanning. (d) The simulation results of detecting the cracks in different directions.

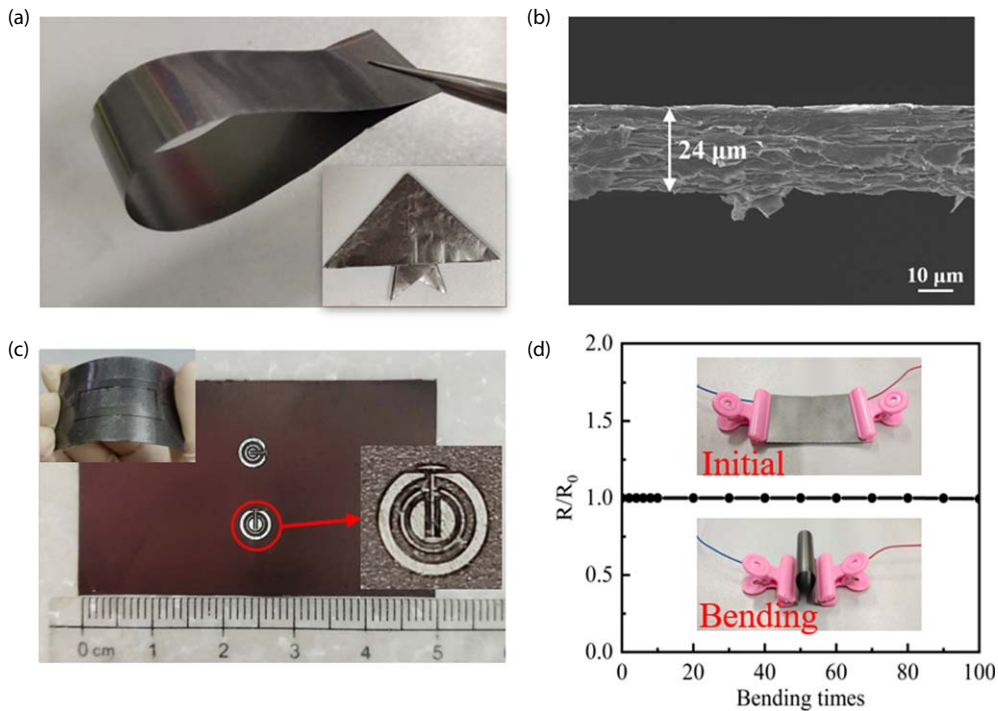


Fig. 5. (Color online) (a) The digital photo of GAF. (b) Cross-sectional SEM image of GAF. (c) The GAF sensor array. (d) Stability test of GAF.

sensor array has good flexibility. In order to further explore the mechanical stability of GAF, the fatigue resistance of GAF is tested, as shown in Fig. 5(d). After 100 times bending test, the resistance of GAF remains constant.

As a demonstration, the flat and curved aluminum plates with a crack are tested using the GAF sensor array. The width

and depth of the crack are 0.2 mm and 2 mm, respectively. The digital photo of a flat aluminum plate with a thickness of 5 mm is shown in the vignettes in Figs. 6(a) and 6(b). As shown in the measurement scanning results of the crack location in Fig. 6(a), when the crack is located in the center of the resonant structure, the resonant frequency offset is the

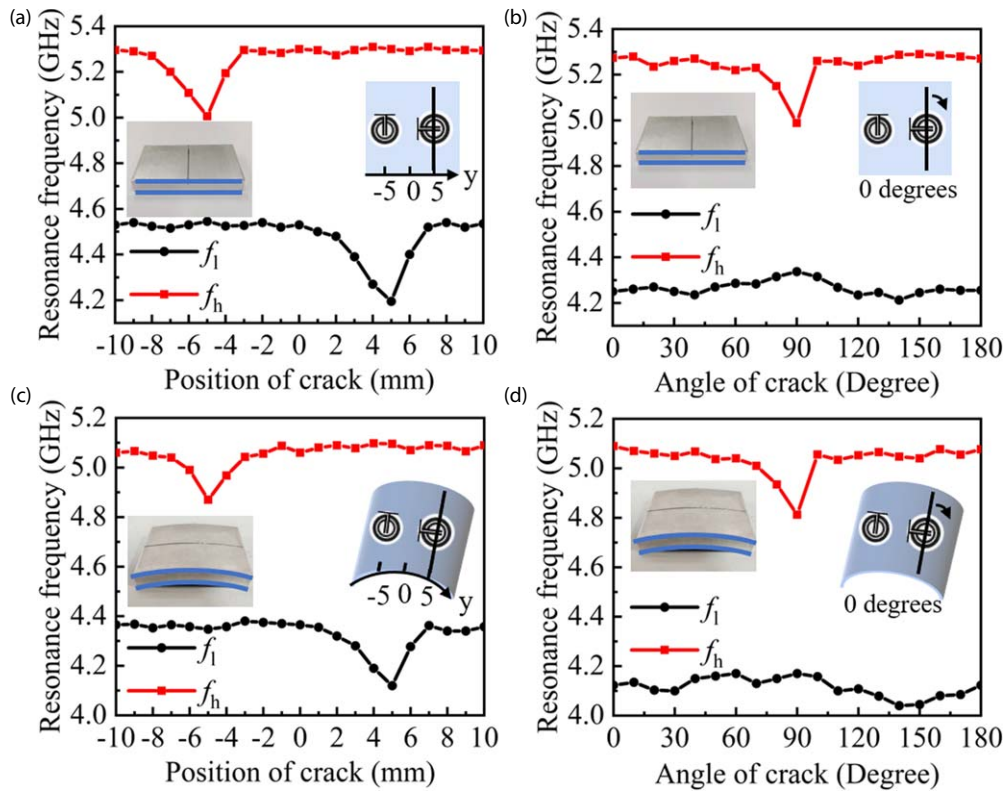


Fig. 6. (Color online) (a), (b) Detection of crack location (a) and direction (b) on flat aluminum plate. (c), (d) Detection of crack location (c) and direction (d) on curved aluminum plate.

Table II. Properties comparison of crack sensors in this work and references

References	Crack width/Frequency shifts	Sensitivity (MHz mm ⁻¹)	Judging crack direction	Metal structures
6)	0.2 mm/400 MHz	/	No	Flat structure
7)	0.2 mm/260 MHz	/	No	Flat structure
10)	0.1 mm/220 MHz	/	No	Flat structure
12)	0.01 mm/120 MHz	/	No	Curved structure
9)		45	Yes	Flat structure
19)		36.82	Yes	Curved structure
This work	0.2 mm/270 MHz	1350	Yes	Curved structure

largest, which can indicate the location of the crack in the center of the resonant structure S_1 . Figure 6(b) shows the influence of the crack on the resonant frequency of the GAF sensor array in different directions. When the crack direction changes from 0° to 180°, the resonant frequency f_h will shift significantly when it passes under the resonant structure S_2 . Therefore, the crack direction can be determined. The test results of the flat aluminum plate are consistent with the simulation results. The digital photo of the curve aluminum plate with a bending radius of 100 mm is shown in the vignettes in Figs. 6(c) and 6(d). Figures 6(c) and 6(d) illustrate the test results of detecting cracks in different positions and directions on the surface of curved aluminum plates, which are consistent with the above detection results of flat aluminum plates. Therefore, the conformal CSRR derived GAF sensor array with two resonant frequencies can accurately detect the location and direction of the surface crack of flat and curved metal structures.

Table II provides the properties comparison between the crack sensors in this work and references. Compared with the rigid RF sensor based on single resonance in references, the

GAF conformal CSRR derived sensor array can realize the detection and orientation determination of submillimeter cracks on curved aluminum plates. In addition, compared with the sensor in references, the GAF sensor array has a higher detection sensitivity for minimal cracks.

In conclusion, a GAF conformal sensor based on CSRR derived structure array is proposed. The GAF sensor array can not only detect the position and direction but also detect the depth and width of cracks on planar and curved metal structures. In addition, the GAF sensor array has a high sensitivity for the submillimeter crack, with a frequency offset of up to 270 MHz for the curved aluminum plate with a crack of 0.2 mm width. The design of the GAF conformal RF sensor array provides a new method for detecting the direction of a crack.

Acknowledgments This research was funded by the National Natural Science Foundation of China (No. 51701146 and 62001338), Wuhan Application Foundation Frontier Project (Grant No. 2020020601012220), and the Fundamental Research Funds for the Central Universities (WUT: 205209016 and 20201B005).

ORCID iDs Daping He <https://orcid.org/0000-0002-0284-4990>

- 1) K. Hectors and W. De Waele, *Metals* **11**, 204 (2021).
- 2) R. Wang, Q. Wu, F. Yu, Y. Okabe, and K. Xiong, *Struct. Health Monit.* **18**, 869 (2019).
- 3) K. Fukuoka and R. Hasegawa, *Int. J. Appl. Electromagn. Mech.* **59**, 1267 (2019).
- 4) J. Kim and S. Park, *J. Intell. Mater. Syst. Struct.* **29**, 3396 (2018).
- 5) I. Mohammad and H. Huang, *Adv. Struct.* **14**, 47 (2011).
- 6) A. Ambika, C. Tharini, and T. Ali, *Wirel.* **118**, 2885 (2021).
- 7) Y. Xu, L. Dong, H. Wang, X. Xie, and P. Wang, *Sens. Rev.* **40**, 81 (2020).
- 8) Z. Xie, G. Wang, L. Sun, Y. Li, and R. Cao, *IET Microw.* **13**, 2061 (2019).
- 9) A. M. Albishi, M. S. Boybay, and O. M. Ramahi, *IEEE Microw. Wirel. Compon. Lett.* **22**, 330 (2012).
- 10) H. Dong, W. Kang, L. Liu, K. Wei, J. Xiong, and Q. Tan, *Meas. Sci. Technol.* **30**, 045103 (2019).
- 11) T. Yun and S. Lim, *Sens. Actuator A Phys.* **214**, 25 (2014).
- 12) A. Salim, A. H. Naqvi, A. D. Pham, and S. Lim, *IEEE Access* **8**, 151804 (2020).
- 13) Z. Wang, X. Yang, X. Zhou, P. Su, and J. Wang, *IEEE Sens. J.* **22**, 5662 (2022).
- 14) R. Ding et al., *J. Alloys Compd.* **764**, 1039 (2018).
- 15) G. Xin, T. Yao, H. Sun, S. M. Scott, D. Shao, G. Wang, and J. Lian, *Science* **349**, 1083 (2015).
- 16) N. Zhang, Z. Wang, R. Song, Q. Wang, H. Chen, B. Zhang, H. Lv, Z. Wu, and D. He, *Sci. Bull.* **64**, 540 (2019).
- 17) R. Song, S. Jiang, Z. Hu, C. Fan, P. Li, Q. Ge, B. Mao, and D. He, *Sci. Bull.* **67**, 1122 (2022).
- 18) H. Zu, B. Wu, Y. Zhang, Y. Zhao, R. Song, and D. He, *IEEE Antennas Wirel. Propag. Lett.* **19**, 2354 (2020).
- 19) R. Song, Z. Wang, H. Zu, Q. Chen, B. Mao, Z. P. Wu, and D. He, *Sci. Bull.* **66**, 103 (2021).
- 20) S. Jiang, R. Song, Z. Hu, Y. Xin, G. Huang, and D. He, *Carbon* **196**, 493 (2022).
- 21) C. Tong, R. Song, H. Guan, Y. Yang, and D. He, *Int. J. Rf. Microw. C. E.* **32**, e23172 (2022).